SLAC-PUB-2944
COLO-HEP-38
May 1982
(T/E)

SOME RECENT RESULTS FROM THE MAC DETECTOR AT PEP*

MAC Collaboration:
Colorado-Frascati-Northeastern-SLAC-Utah-Wisconsin†
Presented by W. T. Ford, Colorado

ABSTRACT

Preliminary results are presented for non-radiative and radiative muon pair production and limits on the production of excited muon states. A new measurement of the tau lepton lifetime is presented. Calorimeter studies of multihadron production are described, with preliminary results for the total and energy-correlation cross section and inclusive muon production rates.

(Submitted to the 5th International Conference
"Novel Results in Particle Physics",
Vanderbilt University, May 24-26, 1982)

---

*Work supported in part by the Department of Energy, under contract numbers DE-AC02-76ER02114 (CU), DE-AC03-76SF00515 (SLAC), and DE-AC02-76ER00881 (UW), by the National Science Foundation under contract numbers NSF-PHY80-06504 (UU), NSF-PHY79-20020, and NSF-PHY79-20821 (NU), and by I. N. F. N.

†MAC Collaborators are: W. T. Ford, J. S. Marsh, A. L. Read, Jr., J. G. Smith, Department of Physics, University of Colorado, Boulder, CO 80309; A. Marini, I. Peruzzi, M. Piccolo, F. Ronga, Laboratori Nazionali Frascati dell' I.N.F.N. (Italy); L. Baksay, H. R. Band, W. L. Faissler, M. W. Gettner, G. P. Goderre, B. Gottschalk, R. B. Hurst, O. A. Meyer, J. H. Moromisato, W. D. Shambroom, E. von Goeler, Roy Weinstein, Department of Physics, Northeastern University, Boston, MA 02115; J. V. Allaby, W. W. Ash, G. B. Chadwick, S. H. Clearwater, R. W. Coombes, Y. Goldschmidt-Clermont, H. S. Kaye, K. H. Lau, R. E. Leedy, S. P. Leung, R. L. Messner, S. J. Michalowski, K. Rich, D. M. Ritson, L. J. Rosenberg, D. E. Wiser, R. W. Zdarko, Stanford Linear Accelerator Center, Stanford University, Stanford, CA 94305; D. E. Groom, H. Y. Lee, E. C. Loh, Department of Physics, University of Utah, Salt Lake City, UT 84112; M. C. Delfino, B. K. Heltsley, J. R. Johnson, T. Maruyama, R. M. Morse, R. Prepost, Department of Physics, University of Wisconsin, Madison, WI 53706.

INTRODUCTION

The MAC detector has been running at PEP for about a year and a half and has accumulated about 24 inverse picobarns of data, at center-of-mass energy 29 GeV. The detector (Fig. 1) which is described in some detail in the proceedings of the 1982 SLAC instrumentation conference[1], is designed to measure the total energy and its angular distribution in a hadron and electromagnetic calorimeter of nearly 4π acceptance. The calorimeter surrounds a large-acceptance drift chamber and solenoid magnet for charged-particle tracking, and is surrounded by drift chambers for muon tracking.

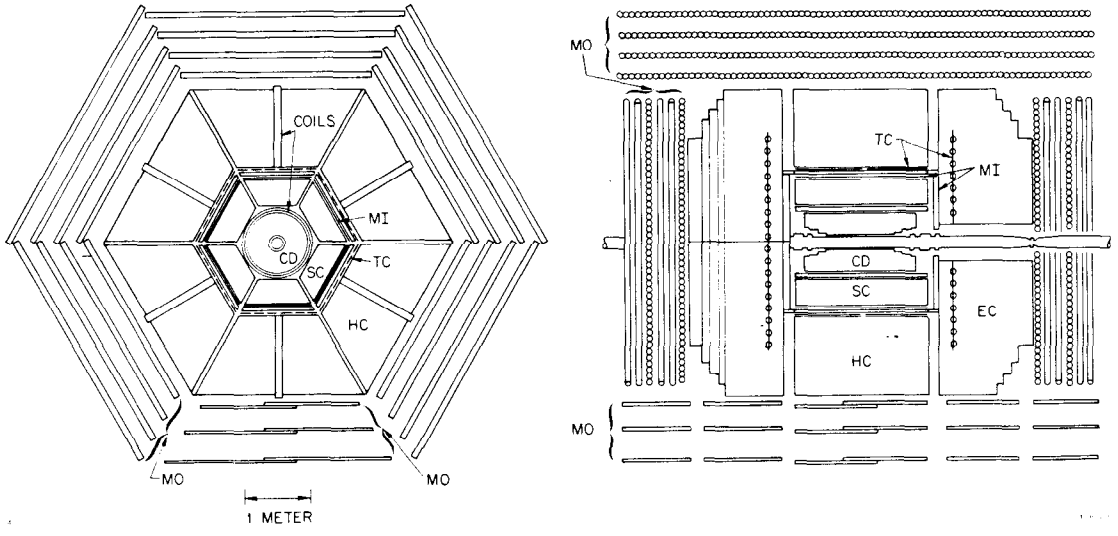

Fig. 1. MAC detector layout. The components labelled in the figure are: central drift chamber (CD), shower chamber (SC), trigger/timing scintillators (TC), central and endcap hadron calorimeters (HC, EC), and the inner and outer muon drift chambers (MI, MO). Also indicated are the solenoid and toroid coils.

COLLINEAR MUON PAIRS

The production of muon pairs is described according to the standard electroweak theory by

$$\frac{d\sigma}{d\cos\theta} = \frac{\pi\alpha^2}{2s}\left[(1+a_1)(1+\cos^2\theta) + 2a_2\cos\theta + \Delta QED(\alpha^3)\right] , \qquad (1)$$

where

$$a_{1,2} = g_{V,A}{}^{e}\, g_{V,A}{}^{\mu}\, \frac{1}{\pi\alpha}\,\frac{G}{\sqrt{2}}\,\frac{-s}{1-s/M_Z{}^2} .$$

Equation (1) includes the contributions of the single photon annihilation diagram and of its interference with annihilation through the neutral weak intermediate vector boson, Z_0. The term $\Delta QED(\alpha^3)$ refers to the radiative corrections to the QED cross section, calculated to order α^3 in reference 2.

The sample consists of those events having two charged prongs forming a vertex in the beam intersection volume which are collinear within 10°, and calorimeter pulse heights along the trajectories that are consistent with either two muons or with one muon and one unresolved muon-plus-photon. Cosmic rays are rejected by requiring that each trajectory intersect a scintillator which produced a pulse with the correct arrival time. The sum of the two muons' momenta is required to be greater than 8 GeV to discriminate against $ee\mu\mu$ events. Events are rejected if the curvature measurement for one of the tracks gives the wrong sign[3], since we want to measure the charge asymmetry. The final sample contains 1239 events, for $\int Ldt \simeq 20$ inverse picobarns.

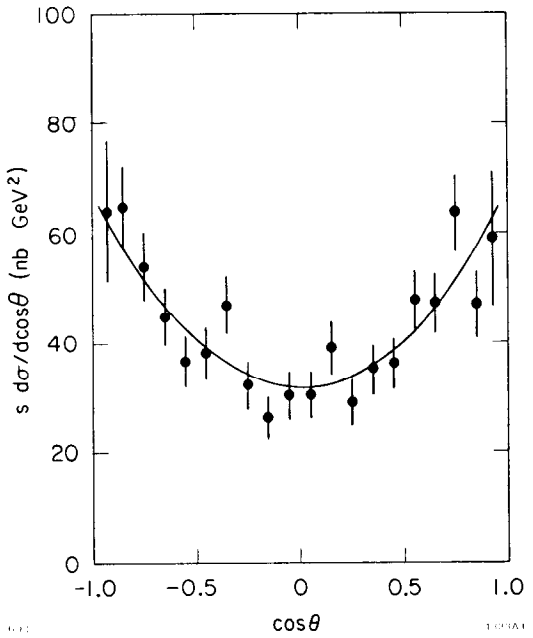

Fig. 2. Differential cross section for μ pair production.

The differential cross section for collinear μμ production is shown in Fig. 2. The curve accompanying the data points was obtained from a maximum likelihood fit of equation (1) to the data with a_2 adjusted. The asymmetry, $A_{\mu\mu}$, is related to a_2 by

$$A_{\mu\mu} = \frac{3}{4} a_2 , \qquad (2)$$

and we find

$$A_{\mu\mu} = -0.032 \pm 0.028 ,$$

which is about one standard deviation from either zero or the standard model prediction of -0.063. The fit χ^2 is 22 for 18 degrees of freedom. This result implies that the product of axial-vector coupling constants is $g_A^e g_A^\mu = 0.13 \pm 0.11$.

HIGHER-ORDER QED AND μ* SEARCH IN μμγ(γ)

By requiring two muons that are non-collinear by at least 10° and one or more observed photons of at least 1 GeV, we select radiative muon pairs which may be used to test the higher-order QED

calculations required, for example, in the weak-electromagnetic asymmetry analysis described in the previous section. Table 1 gives a summary of the $\mu\mu\gamma$ and $\mu\mu\gamma\gamma$ event yields for samples meeting the above criteria and having satisfactory kinematic fits under the appropriate hypotheses. For comparison the prediction of QED calculations including terms of order α^3 (ref. 2) and α^4 (ref. 4) are given for the $\mu\mu\gamma$ reaction. The agreement with the α^4 term included is good. For the $\mu\mu\gamma\gamma$ process we list an estimate obtained by assuming $\mu\mu\gamma\gamma/\mu\mu\gamma \simeq \mu\mu\gamma/\mu\mu$.

	$\mu\mu\gamma$	$\mu\mu\gamma\gamma$
$\int Ldt$ (pb^{-1})	24	12
Events found	133	5
Events expected:		
QED(α^3)	114	—
QED(α^4)	≃138	≃4

Table 1. Summary of event yields and predictions for $\mu\mu\gamma(\gamma)$ events.

The distributions in single-particle energy and production angle are given in Figs. 3 and 4, respectively, together with the predictions from the Kleiss Monte Carlo[2].

Possible deviations from QED in these reactions would include production of excited muon states, μ^*, via the reactions

$$e^+e^- \to \mu^+\mu^{*-}, \quad \mu^{*-} \to \mu^-\gamma \tag{3}$$

$$e^+e^- \to \mu^{*+}\mu^{*-}, \quad \mu^{*-} \to \mu^-\gamma, \quad \mu^{*+} \to \mu^+\gamma \tag{4}$$

In the pair-production process (4), the μ^*s would presumably couple to the virtual photon in the same manner as muon pairs, except for a possible form factor. Reaction (3) could proceed via a tensor coupling

$$\lambda e \sigma_{\mu\nu} F^{\mu\nu} ,$$

which for μ^* mass M leads to the cross section[5]

$$\frac{d\sigma}{d\Omega} = \lambda^2\alpha^2 \frac{(s-M^2)^2}{s^2}\left[(s+M^2)-(s-M^2)\cos^2\theta\right] \tag{5}$$

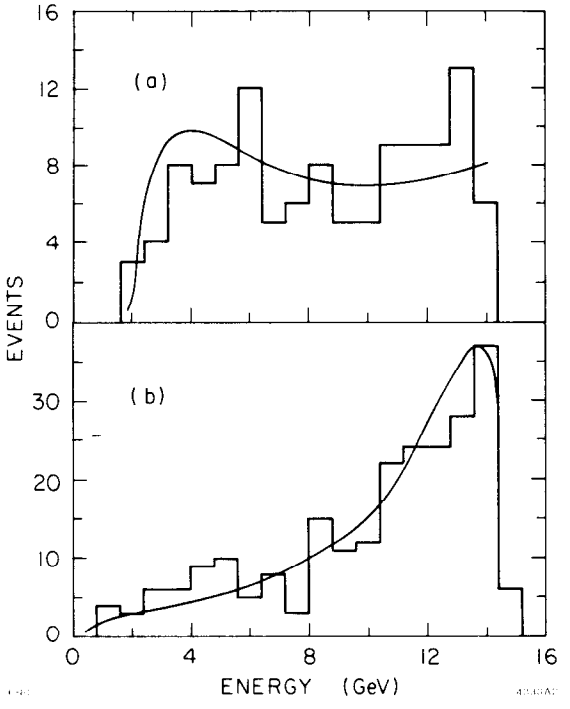

Fig. 3. Energy distributions for (a) photons and (b) muons for $\mu\mu\gamma$ events.

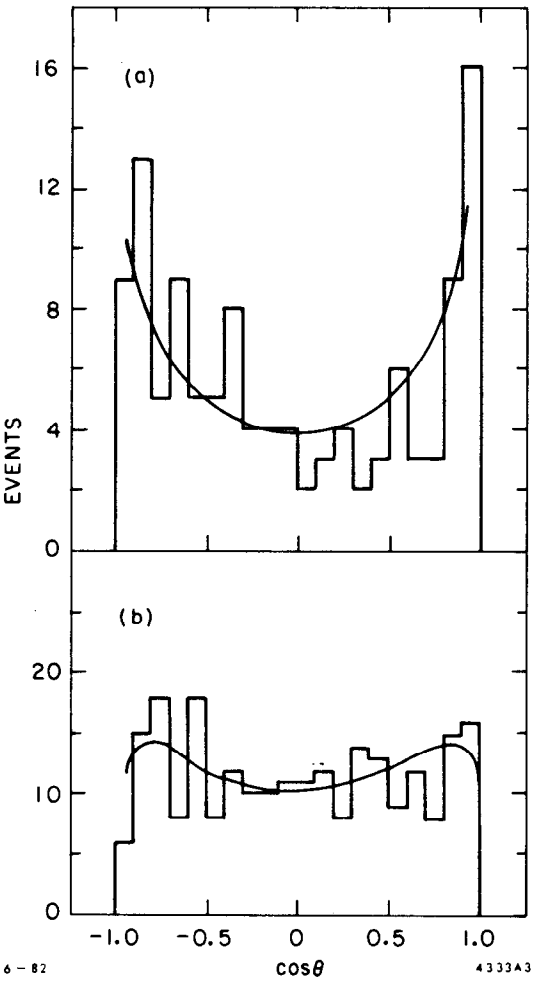

Fig. 4. Polar angle distributions for (a) photons and (b) muons for $\mu\mu\gamma$ events.

Figure 5(a) shows the distribution of the $\mu\mu\gamma$ events in the $\mu\gamma$ mass, together with the QED calculation. The mass rsolution is indicated in Fig. 5(b), the distribution of Monte Carlo events of reaction (3) with mass($\mu\gamma$) = 15 GeV/c^2. The lack of excess events in the data compared with the calculation can be translated into a limit on the production rate of μ^*s for each mass bin, as shown in Fig. 6. The bin width has been chosen to match the resolution.

For reaction (4) we would expect the correct pairing of muons with photons to yield two equal masses. None of our 5 $\mu\mu\gamma\gamma$ events meet this criterion within 2 standard deviations, so we have no candidates. The resulting limit as a function of μ^* mass is plotted also in Fig. 6.

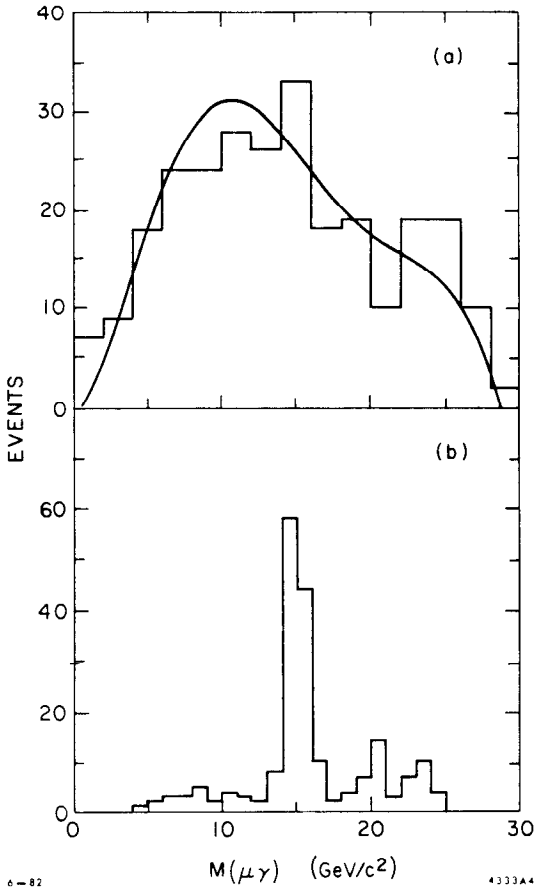

Fig. 5. (a) μ-γ mass distribution for μμγ events. (b) Monte Carlo mass spectrum for μγ from decay of a μ* of mass 15 GeV.

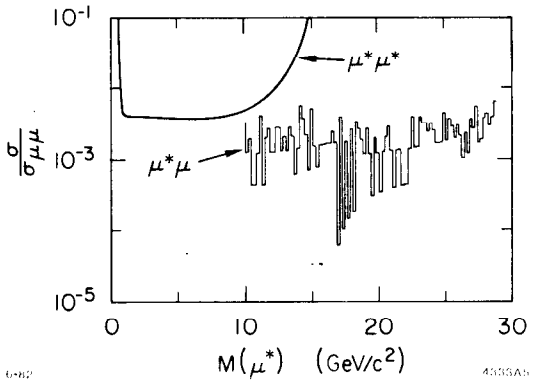

Fig. 6. Upper limits on the cross section relative to the point cross section for production of μμ* (solid histogram) and μ*μ* (dashed curve).

TAU LIFETIME

Tau leptons of 14.5 GeV are expected to travel about 0.7 mm on average before decaying. About 15-20% of the decay final states contain three charged prongs, whose vertex can be localized within about 3-4 mm in our detector. The error on the mean for a sample of N events is, of course, smaller by a factor $\sqrt{N}$, allowing a measurement of interesting significance if N is of order a hundred or more and systematic effects can be controlled.

We selected events having 4 or 6 prongs in narrow jets of 1 or 3 particles, and zero net charge. Each three prong decay candidate was subject to the following track quality conditions: an average of at least 7 hits per track, χ^2 for the vertex fit less than 15 for 3 degrees of freedom, and net charge equal to ± 1. Events passing these criteria were examined visually; about half were rejected as obvious background, mostly single photon or two photon multihadrons, often containing extra unreconstructed tracks.

Remaining backgrounds were: (1) Bhabha electron pairs with an additional pair from conversion of a radiated photon that failed to be reconstructed as such; (2) $ee\tau\tau$ and ee(hadron) events with undetected electrons; (3) beam-gas interactions; and (4) 4- and 6-prong multihadron events.

To remove these backgrounds the following additional requirements were imposed: (1) the total energy computed from the calorimeter pulse heights less than the pure-electromagnetic equivalent of 24 GeV, to eliminate converting radiative electron pairs; (2) charged-track sphericity less than 0.03, which Monte Carlo calculations showed would retain almost all τ pairs while removing a large fraction of beam-gas, $ee\tau\tau$, and ee(hadron) events; (3) the net momentum of each triplet greater than 4 GeV/c to discriminate further against $ee\tau\tau$ events; and (4) the larger of the two jet invariant masses, determined from energy-flow in the calorimeters, less than 4.5 GeV/c^2 (the invariant mass distribution of the visible τ decay products is bounded by $m_\tau \simeq 1.8$ GeV, broadened by the hadron cascade in the calorimeter; from the corresponding distribution for detected multihadron events (see Fig. 7) we found that about 90% were excluded by this cut, independent of their charged multiplicity).

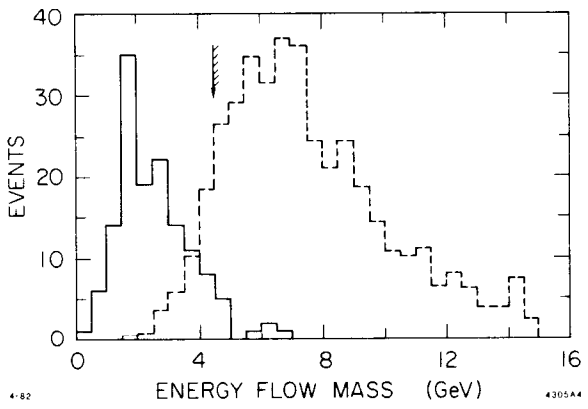

Fig. 7. Mass of the more massive jet for τ candidates (solid histogram and multihadron events (dashed histogram). The multihadron curve is normalized arbitrarily with respect to the τ curve.

From an integrated luminosity of 17 pb^{-1} we found 135 events. Table 2 shows the distribution of these events among the several decay modes of the second τ, together with theoretical estimates[6]. We find generally good agreement, except for an indication of fewer 3-prong and more 1-prong multihadron decays than predicted.

X	theoretical b.r.	theoretical yield	observed yield
e	0.18	23.5	23
μ	0.175	22.9	26
π	0.111	14.5	10
$\pi + n\pi^0$	0.334	43.7	55
3-prong	0.187	24.4	15
	0.987	129.0	129

Table 2. τ decay modes from $e^+e^- \to \tau(\to 3\text{-prong})\tau(\to X)$. The first column lists theoretical branching ratios from ref. 6. The second column entries are branching ratio times 129, to be compared with the observed breakdown of the 129 events for which assignments could be made.

Fig. 8 shows the distribution in calculated error of the flight path. For the decay path distribution of Fig. 9 we include all events for which the error is less than 8 mm. From Fig. 9 we see that the flight path does appear to be non-zero. The calculated mean from Fig. 9(b) is $\langle x \rangle = 1.75 \pm 0.40$ mm. From Monte Carlo calculations we find good agreement with the data if the flight path is taken to be $\lambda = 1.20$ mm; for assumed $\lambda = 0$, we find a bias $\langle x \rangle_b = 0.55$. The stability of this bias against changes in details of the Monte Carlo has been checked. From a study of fake τs selected in various ways from multihadron events we have estimated the systematic error of λ to be 0.3 mm. The result is

$$\lambda = 1.20 \pm 0.39 \pm 0.30 \text{ mm}$$

Combining the statistical and systematic errors in λ and converting to a lifetime value gives

$$\tau_\tau = (4.9 \pm 2.0) \times 10^{-13} \text{ sec},$$

to be compared with the τ/μ unversality prediction of $(2.8 \pm 0.2) \times 10^{-13}$ sec.

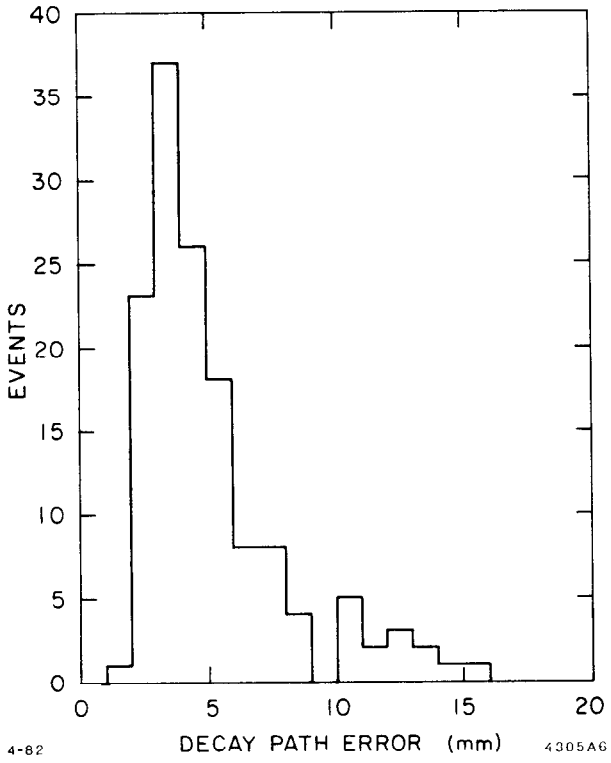

Fig. 8. Distribution of the decay path length error from vertex fits to three-prong τ decays.

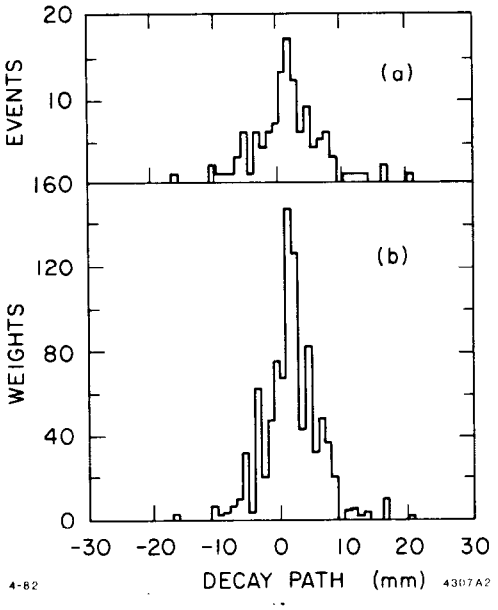

Fig. 9. Decay length distribution for τ decays; (a) unweighted; (b) weighted by the reciprocal squared error.

HADRONIC CROSS SECTION (R)

The ratio R of the cross sections of ee→hadrons to ee→μμ is expected to deviate from the simple quark model prediction (3 2/3 at PEP energies) due to gluon radiative corrections, in a way calculable with quantum chromodynamics (QCD). The first order correction term is expected to be approximately 5%. A measurement of R with sufficient accuracy would be another important test of QCD. The nearly complete solid angle acceptance and calorimetric measurement of the total hadron energy make the MAC detector well suited to a precision measurement of R.

The primary difficulty involved in this measurement is to separate the one-photon annihilation signal from a large background dominated by two-photon annihilation. This is illustrated in Fig. 10, which shows the total energy distribution for a sample of events with at least five reconstructed tracks originating from a common vertex, consistent with coming from the interaction point. The low energy two-photon background is separated out by taking advantage of the fact that these processes tend to have a relatively

large net momentum along the beam direction and a small total momentum transverse to the beam. Thus we define an energy imbalance vector

$$\vec{\beta} = \sum E_i \hat{n}_i / \sum E_i \ , \qquad (6)$$

and transverse energy

$$E_\perp = \sum E_i \sin\theta_i \ , \qquad (7)$$

where the sums are over individual calorimeter hits with energy E_i, polar angle θ_i, and unit vector direction $\hat{n}_i$. Appropriate cuts in these quantities result in the signal (dashed line) and background (dotted line) separation of the events in Fig. 10. Except for events with jet axis very near the beam axis, essentially all single-photon-annihilation events survive the selection process, as one can infer from Fig. 11, which shows the thrust-axis angular distribution.

The results for a sub-sample of the data representing an integrated luminosity of 5.5 pb^{-1}, give the value

$$R = 4.1 \pm 0.05 \pm 0.3 \ .$$

The total systematic error contains nearly equal contributions from event selection, luminosity measurement, and acceptance and radiative correction calculations. A value of 3.9 is expected from QCD with lowest order radiative corrections and α_s=0.17. This result is still very preliminary and we expect the systematic errors to decrease substantially in the near future.

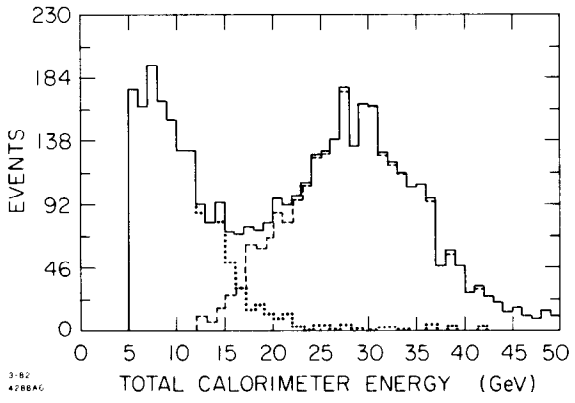

Fig. 10. Total energy for all ≥5-prong events. The dashed histogram represents events passing the selection criteria for multihadron events; events in the dotted histogram are the remainder.

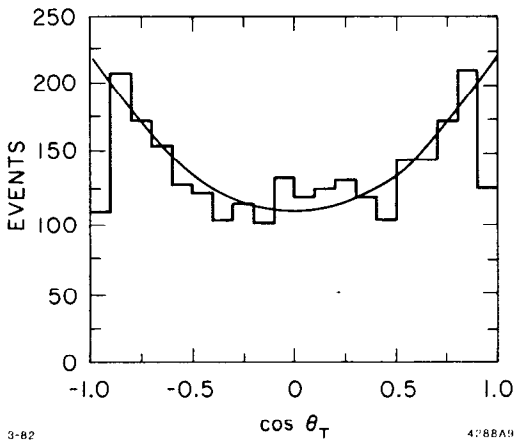

Fig. 11. Angular distribution of the thrust axis for multihadron events, determined from calorimeter energy.

ENERGY CORRELATIONS

Considering hadron production in more detail, a useful approach is to study the angular distribution of the final-state energy, or the "antenna pattern". The energy-weighted cross section can be computed in QCD and is free of divergences. The jettiness is measured by the energy correlation[7],

$$\frac{1}{\sigma}\frac{d\Sigma}{d\cos\chi} = \frac{1}{N\cdot\Delta\cos\chi}\sum_{n=1}^{N}\sum_{i,j}\frac{E_iE_j}{W_n^2}, \qquad (8)$$

where σ is the total cross section, χ is the angle between energy parcels i and j of energy E_i and E_j, N is the number of events and W_n the visible energy of event n ($W_n^2 = s$ for an ideal detector). The second sum is over all pairs having angular separation in the range $\Delta\cos\chi$ about χ.

In zeroth order (parton model), where events consist of two collinear jets, the correlation cross section reduces to delta functions at $\cos\chi = 1$ (self-correlation) and -1 (opposite-parton correlation). Single gluon emmision spreads the two peaks. Since the gluon usually makes a small angle with the quark that radiated it, we get a contribution near $\chi = 0$ from the correlation between this quark and the gluon. At comparable nearness to 180° we get contributions from the correlation of the second (anti-)quark and both the first quark and the gluon, so the cross section is larger in the backward than the forward hemishphere. (The self-correlations still feed the δ-function, so the calculation is not taken too close to $\cos\chi = \pm 1$.)

Fragmentation of the partons leads to contributions of comparable magnitude to single-gluon radiation. The authors of ref. 7 give an estimate of the dominant part of the fragmentation by considering two jet events, i.e., creation of two collinear partons followed by their fragmentation:

$$\left.\frac{1}{\sigma}\frac{d\Sigma}{d\cos\chi}\right|_{frag} = \frac{C\langle h_\perp\rangle}{\sin^3\chi} \qquad (9)$$

Regardless of the specific form of equation (9), the fragmentation to this order is symmetric in $\cos\chi$, which suggests that the asymmetry,

$$A(\cos\chi) = \frac{1}{\sigma}\left[\frac{d\Sigma}{d\cos\chi}(\pi-\chi) - \frac{d\Sigma}{d\cos\chi}(\chi)\right], \qquad (10)$$

is a particularly clean measure of the QCD effects.

The preliminary result of this experiment for the correlation cross section is shown in Fig. 12. The data have been corrected for resolution and acceptance effects determined with a Monte Carlo calculation. The sample was restricted to events having thrust axis at least 30° away from the beam axis to avoid the detector's blind spots near the poles. The solid curve in Fig. 12 is the sum of first-order gluon radiation, quark fragmentation and initial-state photon radiation contributions and is the result of fitting over the range $-.8 \leq \cos\chi \leq .8$, to the data adjusting α_s and the fragmentation coefficient, $C\langle h_\perp \rangle$. One can see from Fig. 12 that we get a poor fit. We may take the point of view that the discrepancy is to be blamed on the fragmentation model and try fit to the asymmetry, as shown in Fig. 13. In this case we get a good fit with $\alpha_s = 0.22 \pm 0.01$ (statistical error only). Systematic detector biases are still being studied.

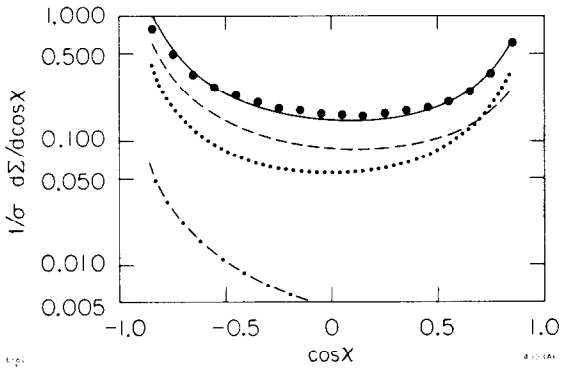

Fig. 12. Energy-correlation cross section. Dashed curve: QCD prediction from Ref. 7; dotted curve: fragmentation contribution; dot-dashed curve: radiative correction; solid curve: sum of all contributions.

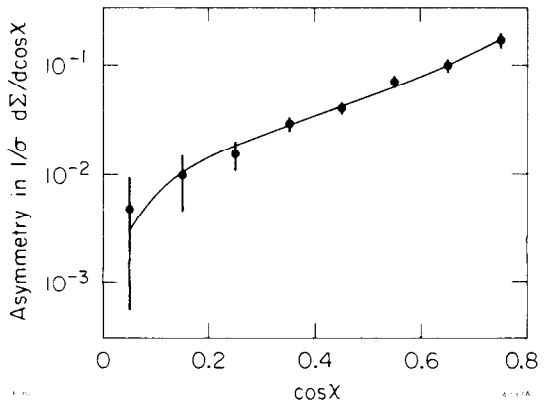

Fig. 13. Asymmetry of the energy-correlation cross section. The curve is the result of a fit of the QCD prediction to the data ($\alpha_s = 0.22$).

More careful consideration shows that the fragmentation contribution will not be exactly symmetric, since fragmentation smearing of a three-jet event adds to the near-forward region from the correlations within each jet, but very little to the corresponding backward region. Instead, the interjet correlations merely smear the region already contributed by gluon emission. This effect may be considered to be higher order than α_s since it involves both gluon emission and fragmentation. In any case, the conclusive confrontation between experiment and QCD awaits a better understanding of fragmentation and probably higher-order QCD calculations as well.

$e^+e^- \rightarrow \mu$ + HADRONS

Multihadron events which include identified leptons can be used for a variety of interesting physics objectives, which include: (1) measurement of the lifetime of the lightest meson containing b quarks (B), thereby obtaining information on the weak mixing angles; (2) measurement of a forward-backward asymmetry of large transverse momentum muons, which, for a pure b quark signal, would be expected to be a factor of three larger than the lepton pair asymmetry since the size of the asymmetry varies inversely as the parton charge; (3) measurement of the branching ratio for $B \rightarrow \mu + X$; (4) measurement of the fragmentation functions of heavy quarks; (5) search for production of new heavy quarks. Though the majority of this physics requires much larger data samples than are currently available, we give here a preliminary report on the status of our inclusive muon analysis and show our sensitivity to item (5) above.

Several features of the MAC detector are very favorable for obtaining a sample of multihadrons containing muons with low backgrounds from decay or punch-through of charged π or K mesons. The detector is compact, therefore minimizing the probability that a π or K decays before it interacts in the calorimeter. In addition, the matching of information in the central drift chamber, inner muon chambers, and outer muon chambers results in a poor χ^2 for most tracks resulting from K decays. Finally, punch-through background can be reduced to a very low level by examining the lateral spread and energy deposition of the track going through the hadron calorimeter.

A sample of multihadron events including an apparent muon was selected by requiring a visible track in the outer muon drift chambers (only those chambers covering 62% of the solid angle could be used for this analysis) correlating with a track in the hadron calorimeter which is μ-like in energy deposition and number of struck channels. Muon track information from the central and inner muon drift chambers is not yet used for this analysis. The momentum of each muon is determined by linking the outer muon chamber track with the interaction position measured by the central drift chamber, and the transverse momentum found relative to the thrust axis for the event. The $p_\perp$ distribution of 219 events from 2/3 of the total data sample is shown in Fig. 14 along with Monte Carlo

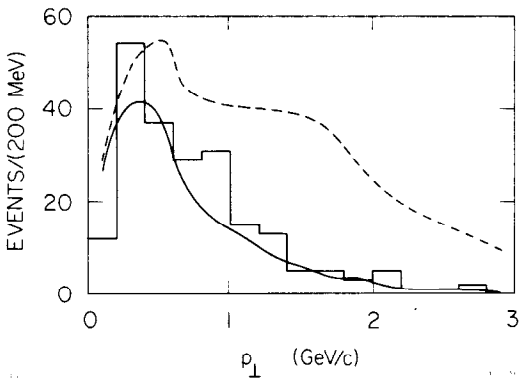

Fig. 14. Momentum perpendicular to the thrust axis for muons in multihadron events. Solid curve: calculated contribution from π, K, c, and b decay. Dashed curve: contribution of a 10-GeV t-quark with 10% muonic branching ratio.

calculated predictions including all known particles (solid curve) and adding a hypothetical sixth quark (dashed curve) of mass 10 GeV and charge 2/3 with a 10% branching ratio to muons. We can therefore exclude at the 95% confidence level the existence of such a new quark with a mass $m_q < 13.5$ GeV. Approximately 40% of the 50 events with $P_\perp > 1$ GeV/c are expected to result from the semileptonic decay of B mesons, while the remainder are roughly equally split between the semileptonic decays of charmed particles and background from π or K mesons.

REFERENCES

1. MAC Collaboration (W. T. Ford, et al.), SLAC-PUB-2894 (to be published in Proceedings of the 1982 International Conference on Instumentation for Colliding Beams, SLAC, edited by W. Ash).

2. The QED cross section is obtained from the Monte Carlo program described by F. A. Berends and R. Kleiss, Nucl. Phys. B177, 237 (1981), and includes all diagrams to order α^3.

3. Reconstruction in the outer drift chambers, which measure the bending of muons in the toroidal magnetic field of the calorimeter, was not yet available for the present analysis. For the central drift chamber alone, $\Delta p/p \simeq .85$ at 14.5 GeV/c, and the probability of mismeasuring the sign for one of the two muons is about 14%.

4. Y. S. Tsai, SLAC-PUB-2741 (1981).

5. A. Litke, Harvard University Ph.D. thesis, 1980 (unpublished).

6. F. J. Gilman and D. H. Miller, Phys. Rev. D17, 1846 (1978) N. Kawamoto and A. I. Sanda, Phys. Letters 76B, 446 (1978).

7. C. L. Basham, el al., Phys. Rev. D19, 2018 (1979); L. S. Brown and S. D. Ellis, Phys. Rev. D24, 2383 (1981).